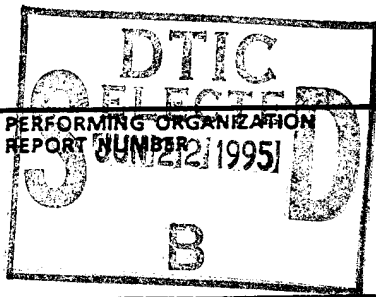# REPORT DOCUMENTATION PAGE

Form Approved
OMB No. 0704-0188

Public reporting burden for this collection of information is estimated to average 1 hour per response, including the time for reviewing instructions, searching existing data sources, gathering and maintaining the data needed, and completing and reviewing the collection of information. Send comments regarding this burden estimate or any other aspect of this collection of information, including suggestions for reducing this burden, to Washington Headquarters Services, Directorate for Information Operations and Reports, 1215 Jefferson Davis Highway, Suite 1204, Arlington, VA 22202-4302, and to the Office of Management and Budget, Paperwork Reduction Project (0704-0188), Washington, DC 20503.

1. AGENCY USE ONLY (Leave blank)	2. REPORT DATE	3. REPORT TYPE AND DATES COVERED
	March 21, 1995	

4. TITLE AND SUBTITLE

ARO Fuel Cell/Battery/Manufacturing HUB Program

5. FUNDING NUMBERS

DAAH04-94-G-0055

6. AUTHOR(S)

Professor Eugene S. Smotkin

7. PERFORMING ORGANIZATION NAME(S) AND ADDRESS(ES)

Illinois Institute of Technology
Chemistry Division
3255 S. Dearborn St.
Chicago, IL 60616

8. PERFORMING ORGANIZATION REPORT NUMBER

DTIC SELECTED JUN 22 1995 B

9. SPONSORING/MONITORING AGENCY NAME(S) AND ADDRESS(ES)

U.S. Army Research Office
P.O. Box 12211
Research Triangle Park, NC 27709-2211

10. SPONSORING/MONITORING AGENCY REPORT NUMBER

ARO 32633.1-CH-HUB

11. SUPPLEMENTARY NOTES
The views, opinions and/or findings contained in this report are those of the author(s) and should not be construed as an official Department of the Army position, policy, or decision, unless so designated by other documentation.

12a. DISTRIBUTION/AVAILABILITY STATEMENT

Approved for public release; distribution unlimited.

12b. DISTRIBUTION CODE

13. ABSTRACT (Maximum 200 words)

The fuel cell program has made progress in four key areas including 1.) fabrication and testing of membrane electrode assemblies (MEAs), 2.) fundamental studies of methanol oxidation on smooth alloy electrodes, 3.) half cell studies of membrane electrode assemblies and 4.) X-ray studies of anode catalytic materials. Two fuel cell test stands with computerized data acquisition systems are now fully operational. We have fabricated MEAs with hydrogen/oxygen performance curves competitive with state-of-the-art electrodes. In addition, studies of Pd barrier electrodes have been initiated and currents of 400 mA/cm^2 at 0.5 volts are typical with hydrogen/methanol-oxygen. We have now terminated the hydrogen/methanol blend experiments and are now focusing on liquid methanol/water feed. We are currently struggling with the methanol delivery system and development of macroporous electrodes for methanol. Since the time of this report, IIT and Argonne National Laboratory have made one visit to the synchrotron at Brookhaven National Laboratory. Data analysis is in progress.

DTIC QUALITY INSPECTED 8

14. SUBJECT TERMS

Fuel Cells, Methanol, Synchrotron, Hydrogen, Membrane Electrode Assemblies

15. NUMBER OF PAGES

33

16. PRICE CODE

17. SECURITY CLASSIFICATION OF REPORT	18. SECURITY CLASSIFICATION OF THIS PAGE	19. SECURITY CLASSIFICATION OF ABSTRACT	20. LIMITATION OF ABSTRACT
UNCLASSIFIED	UNCLASSIFIED	UNCLASSIFIED	UL

ARO FUEL CELL/BATTERY/MANUFACTURING HUB PROGRAM

TECHNICAL REPORT

PROFESSOR: EUGENE S. SMOTKIN
MARCH, 1995

U. S. ARMY RESEARCH OFFICE

GRANT NUMBER : DAAH04-94-G-0055

ILLINOIS INSTITUTE OF TECHNOLOGY

19950620 209

Fuel Cell Program

Table of Contents

ARO FUEL CELL/BATTERY/MANUFACTURING HUB PROGRAM TECHNICAL REPORT

I. FABRICATION AND TESTING OF MEMBRANE ELECTRODE ASSEMBLIES

(Cong Pu)

For establishing methods of fabrication MEAs, we have studied various methods to make conventional $5cm^2$ H_2/O_2 fuel cells with Nafion115 as the electrolyte, 20% Pt on Vulcan XC-72 as the catalyst for both the cathode and anode, and found that the ink/decal transfer method yields a cell with a performance of 1 A/cm^2, at 0.5 V(Fig.1 curve a). Our lab will use the ink technique as the standard method.

Two computer-controlled fuel cell test stations have been set up, which have the ability to deliver up to 60 A. Steady state I-V curves can be measured using home-made software on these stations. The optimum test conditions for different kinds of H_2/O_2 fuel cell systems have been empirically determined. We use 80°C for cells with Nafion electrolytes and 100°C for cell incorporating the Pd barriers.

METHANOL IMPERMEABLE PROTONIC CONDUCTOR (MIPC) ELECTROLYTE

A study of the effect of methanol on fuel cells with and without MIPC electrolyte

I-V curves of fuel cells are measured for the H_2/O_2 fuel cell and with methanol in H_2 fuel stream /O_2 fuel cell. Current-voltage (I-V) curves obtained with a conventional Nafion™ electrolyte suffer a dramatic decrease in OCV, from 1.00 V to 0.77 V, upon addition of methanol to the H_2 fuel stream, with the current density at 0.5 V decreasing within 7 hr from 1050 mA/cm^2 to 330 mA/cm^2 (Figure 2). Degradation of cell performance continues with time.

To prevent methanol crossover, a new composite electrolyte system, a layer of palladium sandwiched between two layers of Nafion, is being developed for fuel cells as an MIPC electrolyte. The I-V curves obtained with the MIPC assemblies reveal that the

open circuit voltages (OCVs) before and after addition of methanol to the hydrogen stream are essentially unchanged (Figure 2). In comparison to Figure 1, where the OCV decreased by 230 mV when methanol was added, with the composite electrolyte system, no OCV drop was observed over a 20 hour period. Only a *slight* decline in the current density is observed for the MIPC system 20 hours after introduction of methanol, compared to a rather drastic reduction in performance of the methanol permeable cells after only several hours, revealing that the lack of crossover prevents poisoning of the cathode electrocatalyst and that only anode poisoning occurs.

After prolonged passage of methanol and hydrogen to the MIPC containing cell, (i), the anode could be reactivated by purging oxygen through the anode compartment ; the I-V curves collected in pure H_2 fuel after oxygen purging were identical to the original data collected in pure H_2 before introducing methanol into fuel cell. This observation further confirms the fact that the MIPC electrolyte prevents methanol crossover avoiding cathode poisoning.

Alternate configurations of the MIPC electrolyte

A variety of configurations for MIPC electrolytes have been tested to gain insights necessary to developed improved electrolytes, such as sputtering Pd on Nafion, sputtering a very thin layer of Pd on a smooth subtract and then transferring the Pd layer to Nafion, and modifying Pd foil surface with sputtered Pt, with evaporated Pt or with electrochemically deposited Pt. Some of I-V curves of fuel cells with differently configured MIPC electrolytes are presented in Fig.3.

The current density obtained with the Pt-modified palladium MIPC is more than an order of magnitude higher than with unmodified palladium cell (ii) at cell potentials greater than 0.5 V. This may be due to the higher proton exchange current density at a platinum surface than at Pd. Increasing the surface area (density of active sites) available for proton exchange and appropriately activating the MIPC surface with a material such as Pt which possesses a high intrinsic exchange current density for hydrogen reductive adsorption/oxidation should improve the performances. Comparison of MIPC cells with interfaces modified with Pt via various techniques such as electrochemical deposition,

2

sputtering and evaporation, indicates that the cell performance is markedly sensitive to the method of interface modification. The sequential electrochemically deposition Pd and then Pt on Pd foil cell (iii) has proven to be the most effective method among them. These differences in performance probably reflect differences in the density of active sites available for proton exchange produced via the different methods.

FURTHER ANALYSIS AND RESEARCH ON THE IMPEDANCE OF MIPC FUEL CELLS

Analysis overpotential on MIPC electrolyte

In order to understand the overpotential produced at each face of the MIPC electrolyte, I-V curves were measured for fuel cells containing the following composite electrolytes: (iv) a Pd foil modified by a surface layer of evaporated Pt upon the side facing the anode, (v) a Pd foil modified in the same way but upon the side facing the cathode, and (vi) a Pd foil modified on both sides(Figure 4). The relative performances of these Pt-modified Pd MIPCs were compared to that of an unmodified Pd foil. For the Pd foils modified on one side only (i.e. cells (iv) and (v)), the I-V performance was poor, although Pt modification upon the side facing the cathode led to marginal improvement at high cell overpotential. With Pt applied to both sides, however, a dramatic increase in I-V performance was observed.

To elucidate further information about the hydrogen exchange interfacial reactions occurring at the respective faces of the MIPC we can apply a simple curve fitting model to the I-V polarization curves shown in Figures 1 and 4. Since the mass transport overpotential and anode overpotential can be neglected at current densities up to several A cm^{-2} for the hydrogen /oxygen fuel cell with a Nafion 115 bilayer electrolyte cell (Figure 1), the cell potential(E) - current density(I) relation for current densities below 1 A cm^{-2} may be expressed by the equation:

$$E_1 = E_0 - b_1 \log(i) - R_1 I \qquad (1)$$

where b_1 represents the Tafel slope for the oxygen reduction reaction, R_1 is the pseudo-resistance including the bulk resistance of two pieces of Nafion 115. E_0 may be further

3

expressed by:

$$E_0 = E_r + b_1 \log (I_0) \qquad (2)$$

where E_r is the reversible potential for the cell and I_0 is the apparent exchange current density for the oxygen reduction reaction.

By fitting curve a in Figure 2 with equation (1), b_1, R_1 and E_0 are calculated to be 0.0392 V/dec., 0.33 Ω cm^2 and 0.837 V respectively. Utilizing this data, cathode activation overpotential as a function of current density can be obtained for the Nafion bilayer cell. It is reasonable to assume that in cells comprising a composite electrolyte system the reaction kinetics at both the anode and cathode of the cell will be the same as that for the respective electrodes in the Nafion bilayer cell. Consequently, the E-I relation for the MIPC electrolyte cell can be expressed as:

$$E_2 = E_0 - I R_1 - b_1 \log(i) - E_{MIPC} \qquad (3)$$

where E_{MIPC} is the total overpotential produced by introduction of the MIPC into the fuel cell. This overpotential includes terms for the bulk impedance of the MIPC and the interfacial impedance between Nafion and the MIPC. Fitting the I-V curves in Figure 4 to equation (3) using the pre-determined values (from Figure 1) for the constants E_0, b_1, and R_1, yields the relationship between E_{MIPC} and current density. This analysis was performed for cells (ii), (iv), (v) and (vi), (see Figure 5).

From comparison of the E_{MIPC} values for cells (ii), (iv) and (v) at the same current density in Figure 5, the effect of Pt modification of the Pd MIPC surface on the overpotential produced at each interface of the MIPC can be determined by subtraction of the respective E_{MIPC} values for cells with Pt on one side only with unmodified Pd e.g. $E_{MIPC}^{(ii)} - E_{MIPC}^{(iv)}$ gives the reduction in overpotential produced by Pt modification of the MIPC facing the anode. Similarly $E_{MIPC}^{(ii)} - E_{MIPC}^{(v)}$ gives the overpotential reduction for the MIPC side facing the cathode. Below 60 mA/cm^2 it was found that:

$$(E_{MIPC}^{(ii)} - E_{MIPC}^{(iv)}) + (E_{MIPC}^{(ii)} - E_{MIPC}^{(v)}) + E_{MIPC}^{(vi)} = E_{MIPC}^{(ii)} \qquad (4)$$

In this current density regime, the relations between E_{MIPC} and current density follow Butler-Volmer characteristics indicative of the reaction kinetics-controlling nature of the

overpotential on the MIPCs. Above 60 mA/cm^2, processes additional to electrode kinetics appear to control the I-V relations for cells with Pt-modification on one side only as the overpotential increases rapidly suggestive of diffusion-limiting behavior. In favorable contrast, for cells (vi) the Pt modification on Pd deduces the kinetic overpotential for proton exchange reaction at Nafion/MIPC interfaces and the cell overpotential increases more slowly with current. Experimental data suggests that it is necessary to modify both Pd MIPC surfaces to increase the performance of the MIPC-containing cells.

A.C. impedance measurement

AC impedance is an effective method to study the bulk impedance, interfacial impedance and electrochemical kinetics impedance of fuel cells and to in situ characterize fuel cell, so far most of the research work published are about SOFC or MCFC.

Ac impedance experiments were conducted at different voltages for Nafion bilayer PEFC and MIPC-containing PEFC to study the impedance on MIPC electrolyte. In the complex-plane impedance spectra of fuel cell only with Nafion bilayer as electrolyte (Fig.6), there is a depressed semicircle at lower frequency region (region III), the width of that semicircle varies with potential, specifically, the lower the cell voltage, the less cell impedance, which may mainly be due to the oxygen reduction impedance. At higher frequency region the impedance does not become important until the cell voltage is lower than 0.9 V, and it seems that there is another semicircle at highest frequency region (region I), which is more clear at low cell potential. As the width of it does not change with the potential, it is reasonable to consider it to be the bulk impedance of electrolyte. The resistance of two layers of Nafion is about 0.2 Ω cm^2.

The complex-plane impedance spectra obtained at cells with MIPC are shown in Fig.7- Fig.9. By fitting the semicircle in region II and III, the interception of impedance spectra on the real axis at high frequency region could be got, which means the bulk resistance of electrolyte could be obtained and is about 0.2 Ω cm^2. The spectra show a charge-transfer semi-circle in region (III), which also becomes smaller as the cell potential decreases. In addition to these, the most obviously difference between these spectra and those in Fig.6 is that the width of semicircles in region (II) of the cell (R_2) with MIPC electrolyte system are much bigger than those with Nafion bilayer electrolyte, apparently,

it is due to the impedance of the MIPC electrolyte. it was also found that in MIPC-containing fuel cells except for Pt-modified on both sides of MIPC, R_2 decreases quickly with the decrease of cell voltage, which has the character of charge transfer resistance, so that it is clear that the Pt-modification has the effect of decrease charge transfer resistance of proton exchange reaction at Nafion/MIPC interfaces. It confirms the results obtained above.
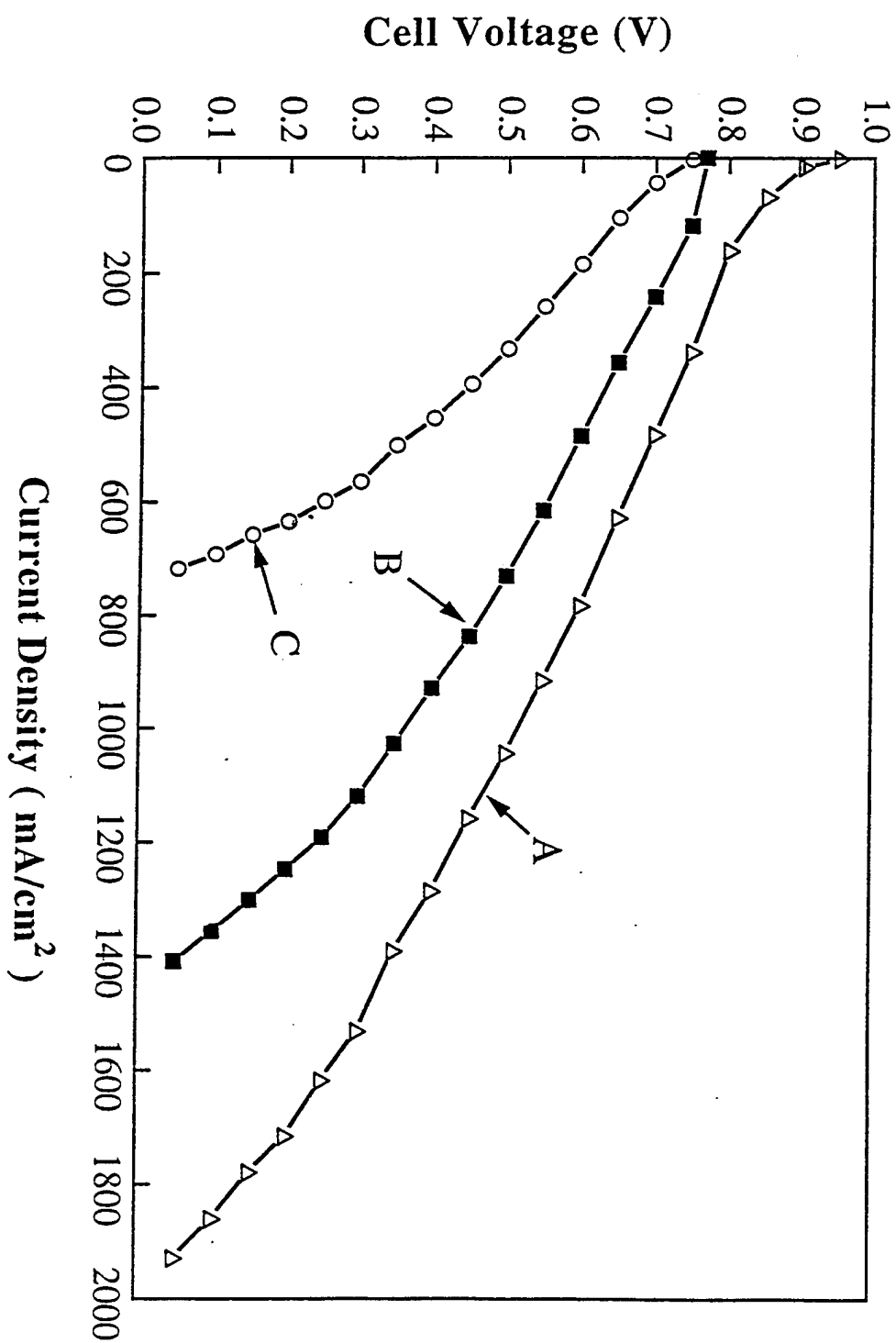
Fig. **1**. I-V curves of a conventional fuel cell with two Nafion™ 115 membranes as the electrolyte. Curve A was obtained with H_2 as the fuel. Curves B and C were obtained 1 and 7 hr., respectively, after adding 12% methanol to the H_2 humidifier.
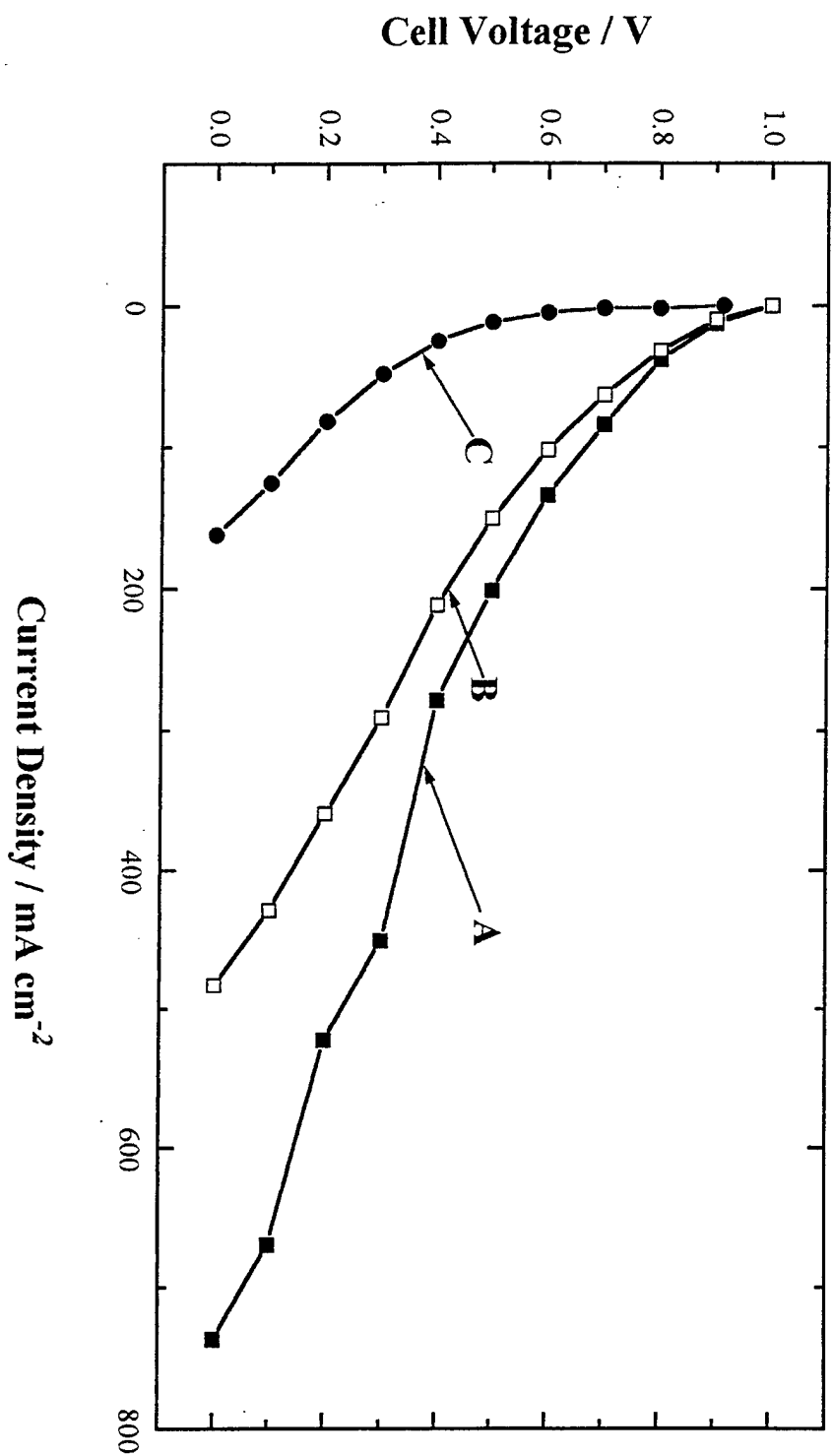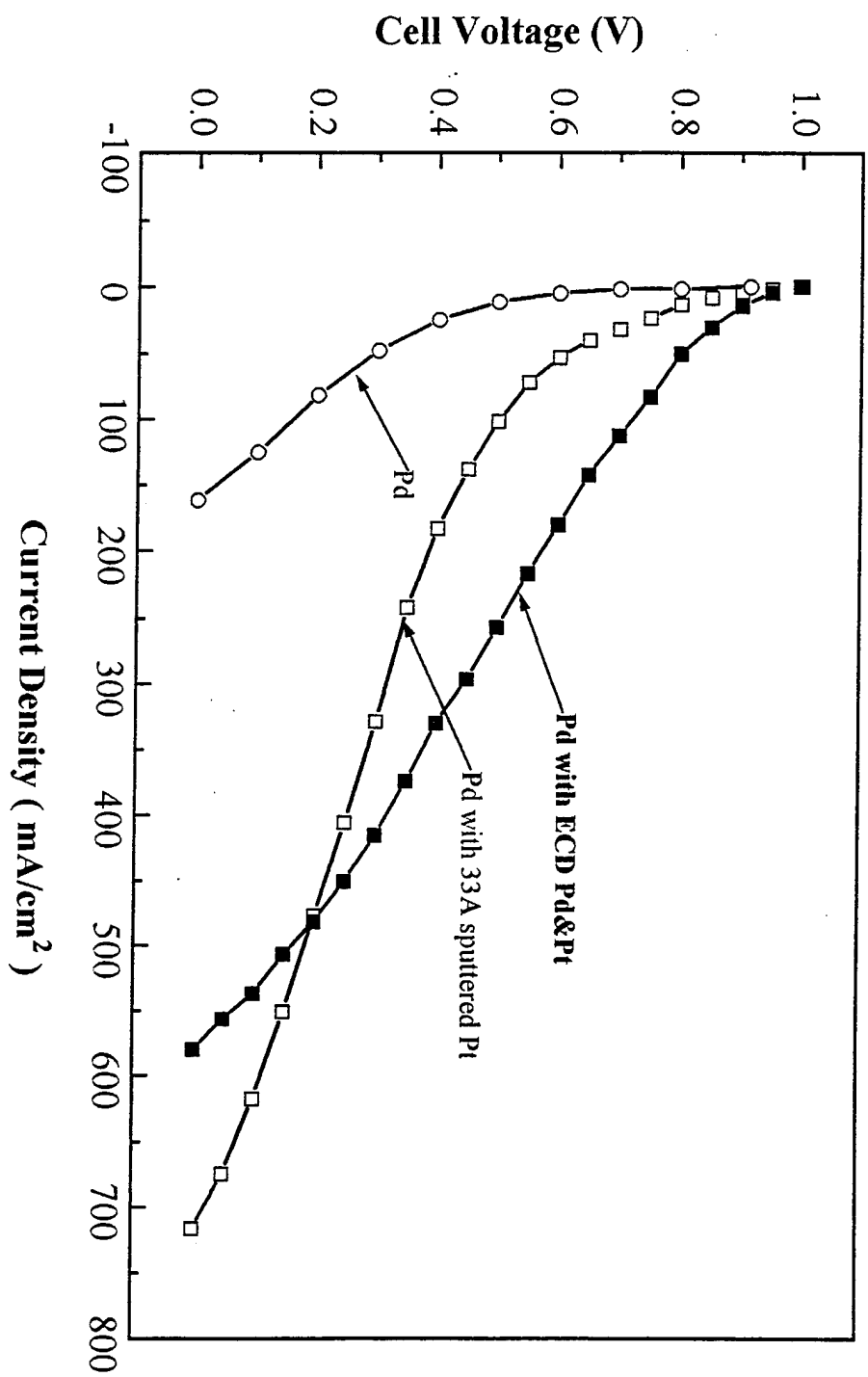
Fig. **2** I-V curves of differently configured fuel cells containing the palladium MIPC sandwiched between two Nafion 115 membranes, which serve as the PPEIs. Curve A was obtained with a palladium foil (25μm) electrochemically deposited with 7 $\mu g/cm^2$ of Pt sandwiched between two Nafion 115 membranes, and H_2 as the fuel. Curve B was obtained 20 hr. after adding 10% methanol to the H_2 humidifier, using the same electrolyte system as in curve A. Curve C was obtained using unmodified palladium foil sandwiched between two Nafion 115 membranes and H_2 as the fuel.

I-V curves of differently configured MIPC contining Fuel cells
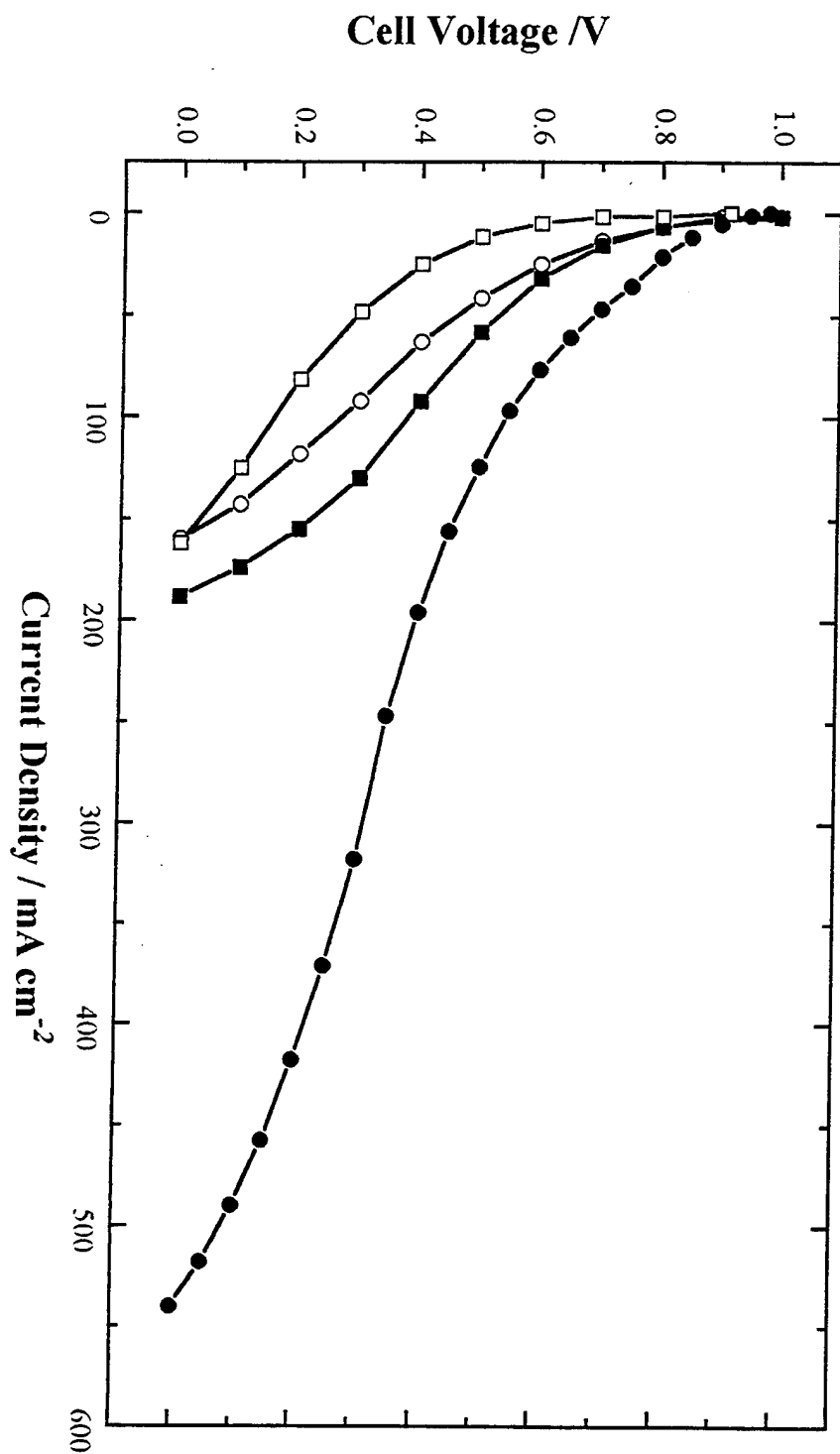
Figure 3

9

Fig. 4. I-V curves of differently configured fuel cells containing the palladium MIPC sandwiched between two Nafion 115 membranes, which serve as the PPEIs. –□–: with unmodified Pd foil; –○–: with a Pd foil modified by a 5 nanometer surface layer of evaporated Pt upon the side facing the anode; –■–: with a Pd foil modified in the same way but upon the side facing the cathode; –●–: with a Pd foil modified on both sides with evaporated Pt.

Fig.5 ────── : with unmodified Pd
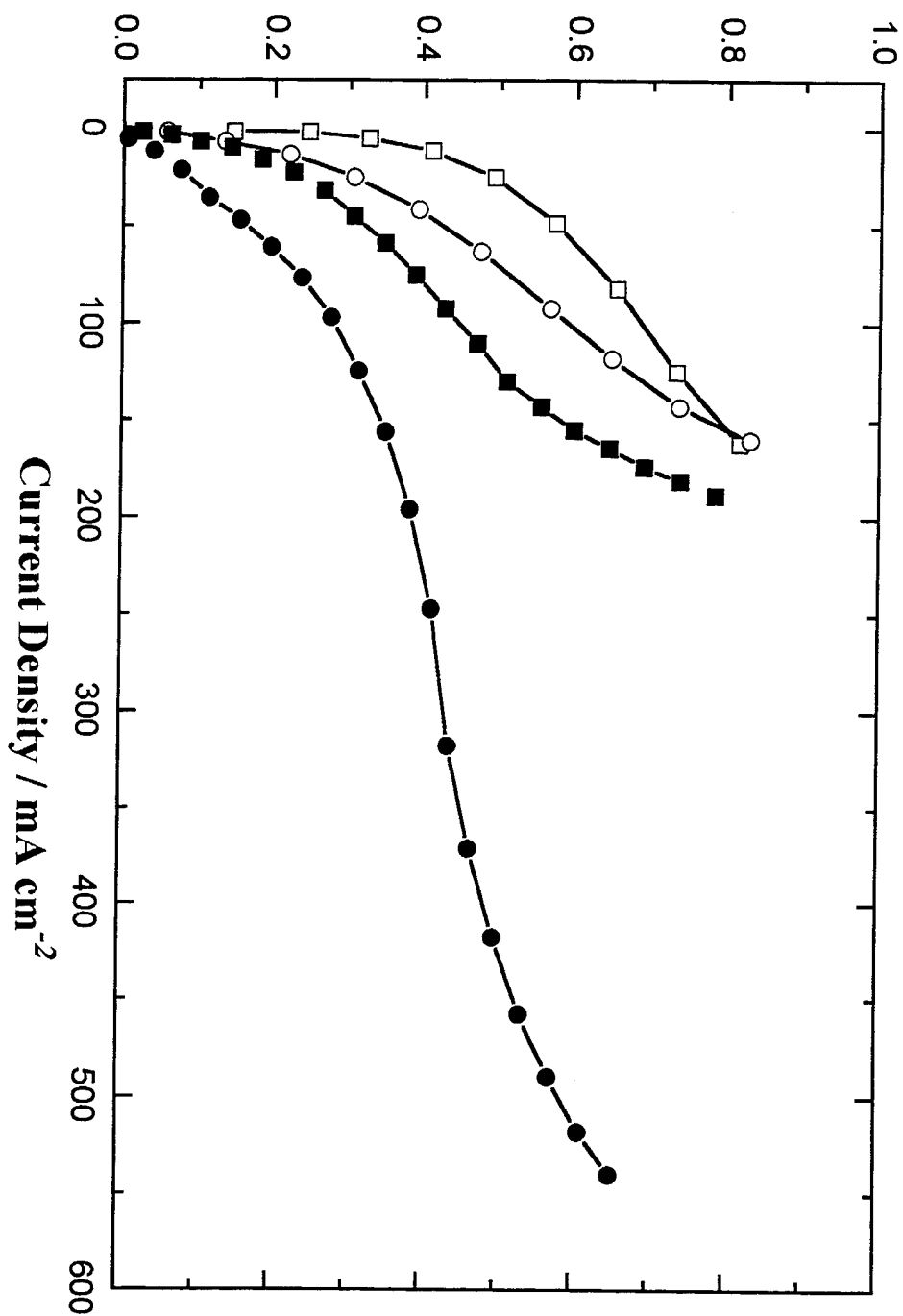────●── : with evaporated Pt on both sides of Pd
────○── : with evaporated Pt on one side of Pd facing anode
────■── : with evaporated Pt on one side of Pd facing cathode
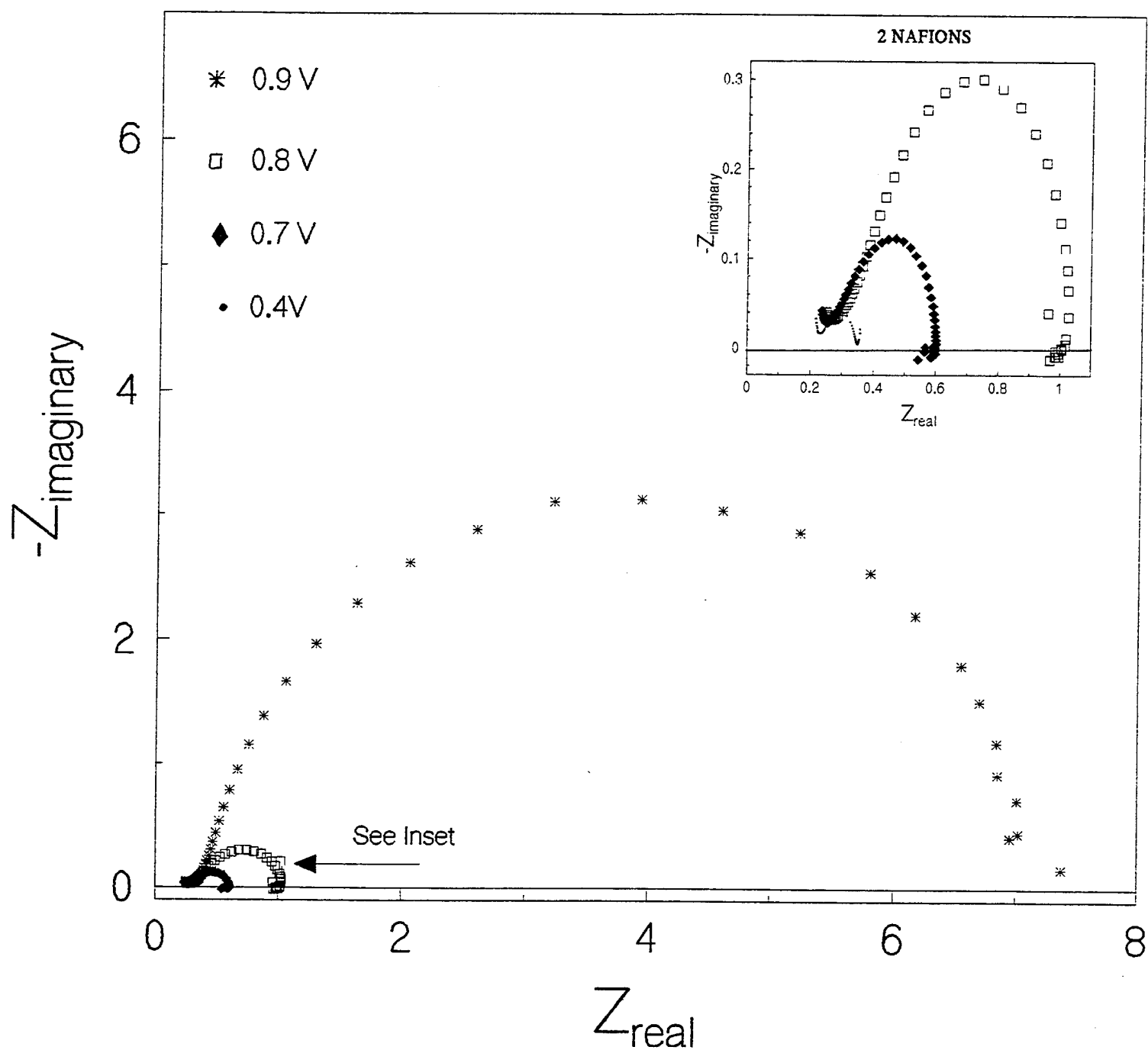
2 NAFIONS

Figure 6

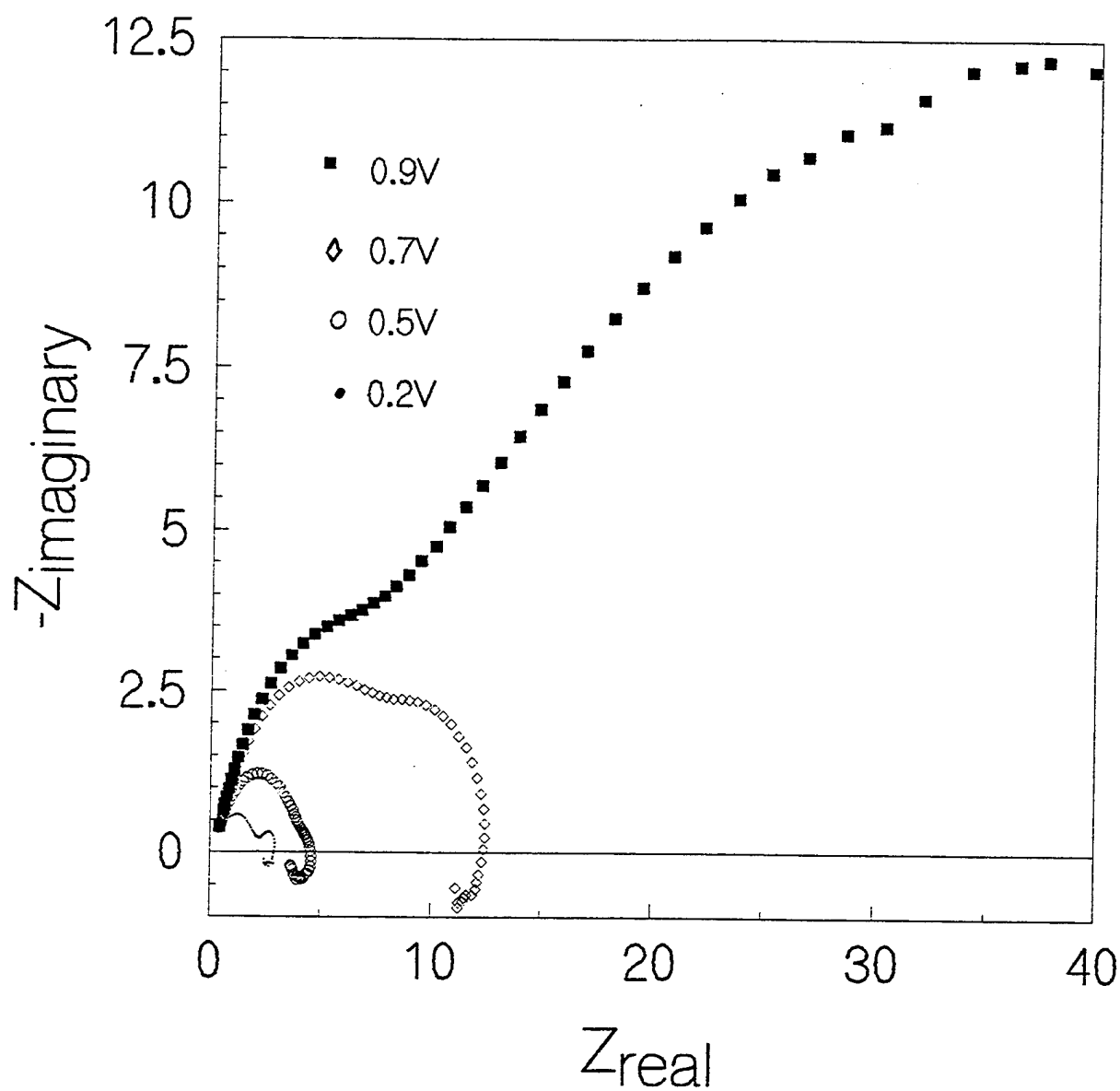# Evaporated Pt on Pd - Anodic side

Figure 7
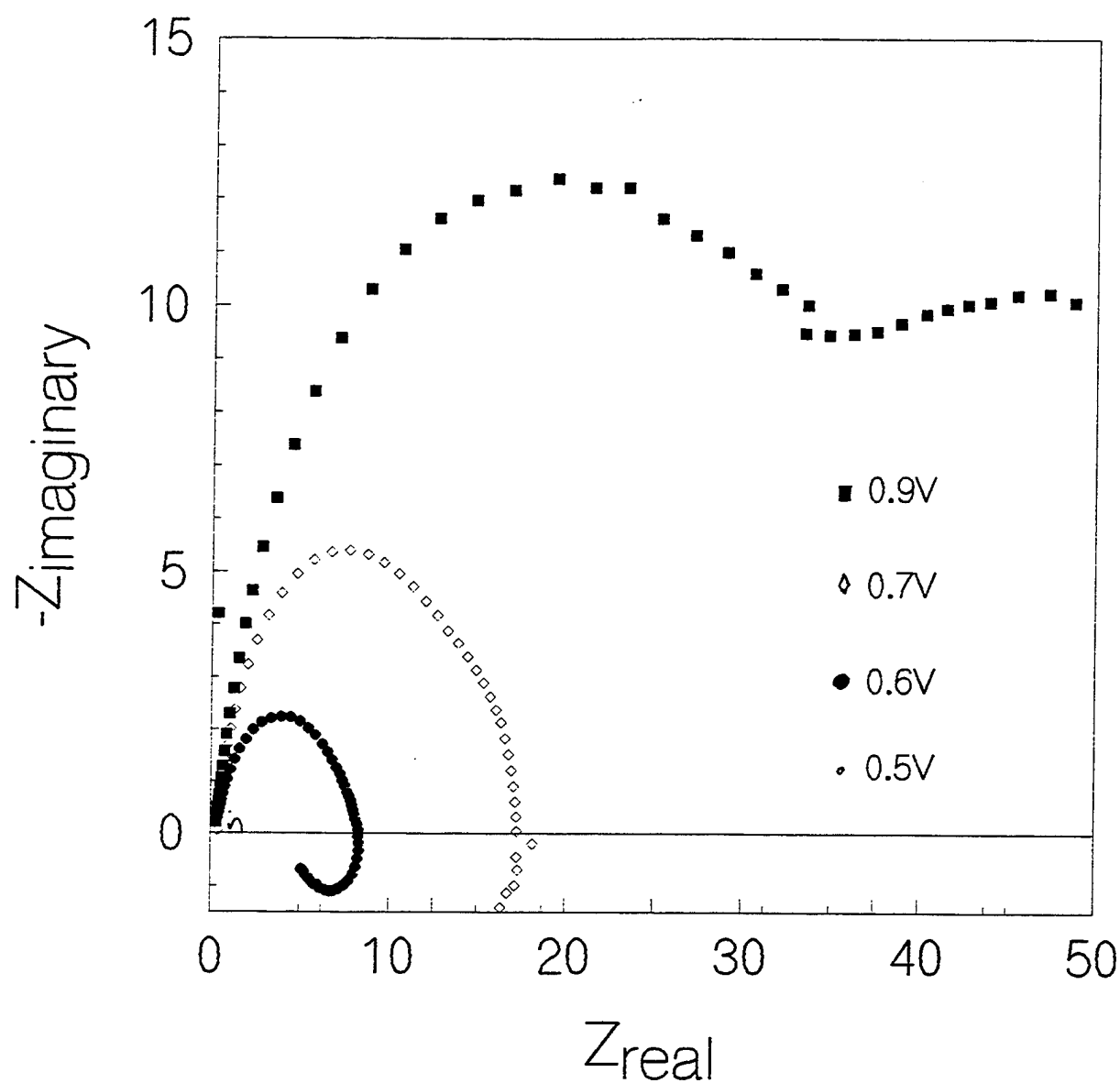
Evaporated Pt on Pd -Cathodic side

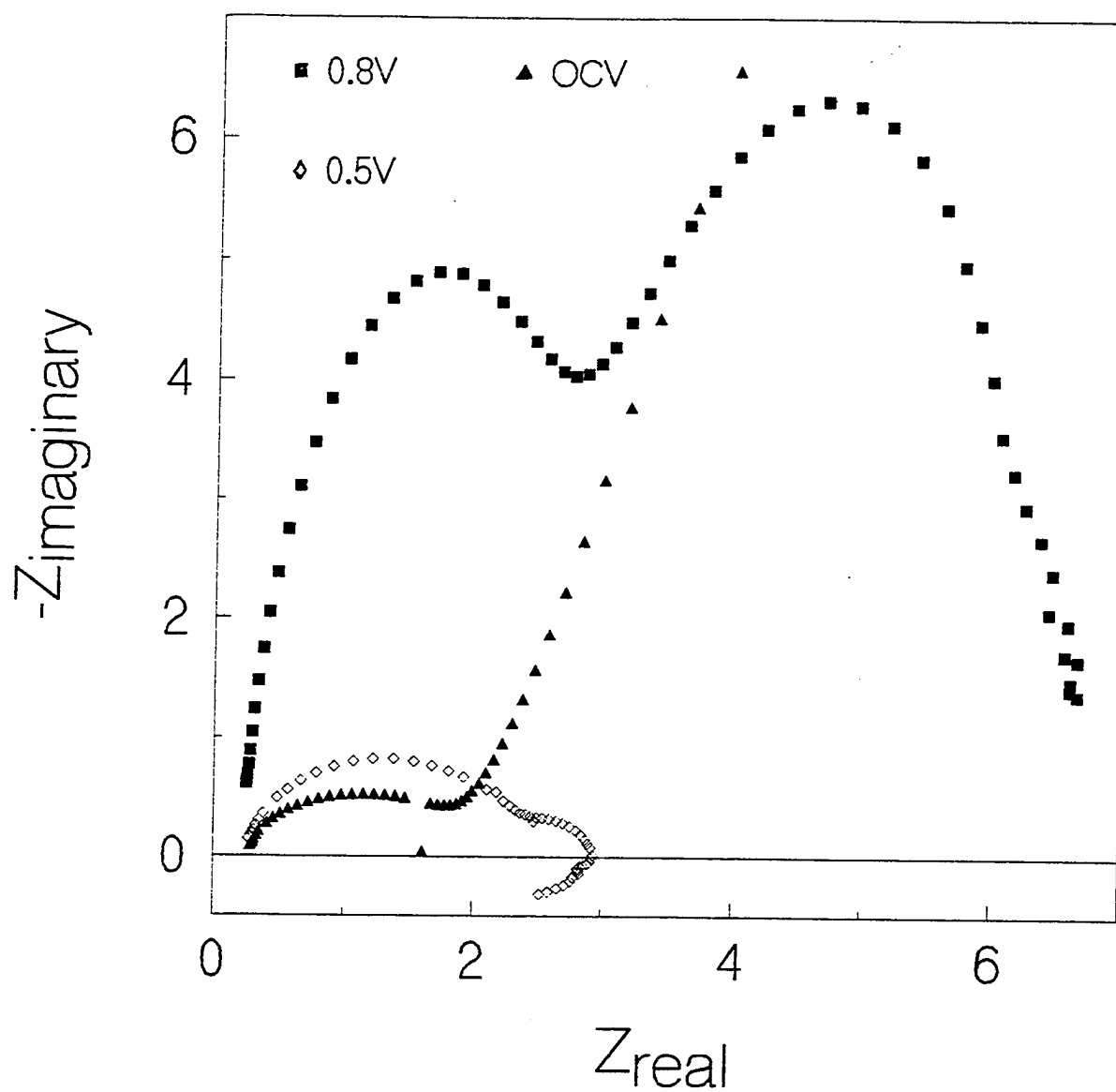

Figure 8

# Evaporated Pt on Pd -Both sides

Figure 9

II. IMPROVED ELECTROCATALYSTS FOR METHANOL ELECTRO-OXIDATION- SMOOTH ELECTRODE STUDIES
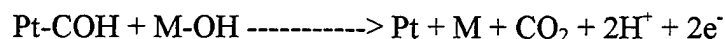
(Kevin Ley)

Introduction

Although Pt is known to possess the highest intrinsic activity for methanol oxidation [Wang, 1992] the catalyst is rapidly poisoned by the partial oxidation intermediate products CO or COH [Beden, 1987, Iwasita, 1992] formed during fuel cell operation. The four electron oxidation product CO tends to predominate at high methanol concentrations, and the three electron oxidation product COH at lower concentrations [Iwasita, 1992]. The rate of removal of these poisoning species has been shown to be enhanced by adsorption of oxygen containing species such as water (i.e. OH) along with methanol fuel molecules [Appleby, 1993a]. Methanol adsorbs on Pt at lower potentials than does water. Although precise details of the catalytic enhancement mechanism have not yet been clarified, Pt-based binary alloys composed of a second metal element with enhanced ability to adsorb water at lower potentials has led to the development of improved electrocatalysts with higher steady-state activities for methanol oxidation; Pt-Ru in fact is widely known to possess the highest steady-state activity for a binary composition [McNicol, 1981, Cameron, 1992]. The search for a suitable alloy system to study is based on the hypothesis that improved methanol oxidation activity can be found by selecting elements to alloy with Pt that adsorb water with sufficient strength so as to promote similar surface coverages of water and methanol at low potentials vs. SHE. This hypothesis assumes that the rate determining step for the oxidation of methanol on alloys involves reaction between water and the -(C,O,H) poison (formed from methanol) to form CO_2, which has been proposed in the literature [Watanabe, 1975, Hampson, 1979, Iwasita-Vielstich, 1990, Arico, 1994]:

At high methanol concentrations:

$$Pt\text{-}CO + M\text{-}OH \text{----------} > Pt + M + CO_2 + H^+ + e^-$$
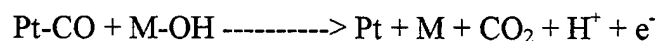
At low methanol concentrations:

$$Pt\text{-}COH + M\text{-}OH \text{ ------------> } Pt + M + CO_2 + 2H^+ + 2e^-$$

Hence, in addition to reaction steps involving transport of reactants (methanol and water) and products (CO_2, H^+, e^-) to and from active sites, the key activated reaction processes are [Bond, 1987a]: adsorption of methanol and water to active sites; reaction on the active sites between the -(C,O,H) poison and water to produce CO_2, protons, electrons and regenerated active sites; desorption of CO_2 from the alloy surface. Since the methanol molecules rapidly decompose to the poisoning intermediate -(C,O,H), the relative strengths of -(C,O,H) binding to Pt and -OH binding to the second metal may be important with respect to the rate of oxidation of the poison. It is interesting to note that in the series of noble metals the strength with which the elements adsorb water follows the strength with which these metals bond with oxygen i.e. written in order of decreasing strength, Os>Ru,Ir>Pt>Rh>Pd [Appleby, 1993b]. An analysis of metal-oxygen bond strengths reveals that the best reported promoter elements, Ru and Sn possess very similar metal-oxygen bond dissociation energies (bond strengths) much higher than for Pt, and that other lesser promoters such as Mo, Re, and Ti possess even higher metal-oxygen bond strengths. Metal-oxygen bond strength data suggests that there may exist an optimum strength at which the second element must bind -OH. These same trends are reflected in heat of chemisorption (adsorption strength) data. Data on the enthalpies of chemisorption of O_2 in kJ/atom O, and CO in kJ/mol on transition metals are available [Bond, 1987b,c]. An approach, therefore, to improved anode compositions may be to develop Pt-based alloys containing alloying components that do not form oxides at the working electrode potential but sorb/bind -OH with similar strength to that of -CO or -COH on the Pt sites of the alloy.

Inspection of available data indicates that Os metal is a good candidate along with the already well studied Ru for alloying with Pt. Os is relatively electropositive, exhibits a metal-oxygen bond strength in the same range as Ru, Sn, Mo, Re and Ti, and exhibits

reasonable solubility (ca. 25 at.%) in Pt [Winkler, 1943, Hutchinson, 1972, Savitskii, 1989]. Additionally, only a few studies [Watanabe, 1972] have been performed for Pt-Os materials with regard to methanol oxidation activity and these do show an enhancement in methanol oxidation activity relative to Pt.

Since the Pt-Ru system is already well studied we propose in addition to binary Pt-Ru and Pt-Os compositions, to study the potentially interesting ternary system Pt-Ru-Os. Observation of the Pt-Ru-Os ternary system indicates that a reasonably extensive region of single phase (face-centered cubic) ternary solid solutions exists at the Pt-rich corner which to our knowledge have not been characterized before with regard to methanol oxidation activity.

Work in Progress

The objective of this component of the HUB program is to map steady-state methanol oxidation activity versus single phase ternary Pt-Ru-Os composition for smooth electrodes and correlate catalytic activity with the known structural features of the various alloys . Polycrystalline binary and ternary single phase solid solutions at the Pt-rich corner of the ternary system (see Figure 10) are being fabricated via arc melting of pellets composed of appropriate proportions of the noble metal powders. X-ray diffraction (XRD), optical microscopy, scanning electron microscopy (SEM) and energy dispersive analysis of x-rays (EDAX) are being used to characterize the bulk alloy structure (single phase, crystal structure, lattice spacings, order-disorder effects) and chemistry (chemical composition). Surface structure will be determined via auger electron spectroscopy (AES), x-ray photoelectron spectroscopy (XPS), and grazing angle extended x-ray absorption fine structure (EXAFS).

At this stage of the program, we can report the successful in-house fabrication of the three polycrystalline binary Pt-Ru electrodes to be studied. XRD patterns of the polished electrodes show a single FCC phase pattern with peaks shifted to higher 2θ values and lattice parameters consistent with Ru substitution into the FCC lattice of Pt (Figure 11).

The alloy pellets are fabricated as disk electrodes for electrochemical studies to be conducted in the temperature range 25-65°C; the disk diameter is machined so that the electrode can be inserted into a Pine rotator. Linear scan voltammetry (LSV), cyclic voltammetry (CV), and rotating ring disk electrode (RRDE) studies will be performed to evaluate the ability of each alloy composition to catalyze the methanol electro-oxidation reaction. Overpotentials for methanol oxidation and resultant oxidation currents will be determined via voltammetry for each alloy composition. In Figure 12, preliminary CV data (using 100 mV/sec scan rate) can be seen for the Pt-20 at % Ru alloy versus Pt in 0.5M H_2SO_4, and 0.5M H_2SO_4/1M CH_3OH solutions respectively. The key differences found with reference to Figure 12 (a) in acid electrolyte are (i) the potential (vs. SHE) at which the resulting noble metal oxide is reduced is shifted to lower positive values for the 20 at% alloy versus Pt, (ii) the hydrogen region of the scan is modified in the sense that for the alloy electrode, the three reductive adsorption and corresponding oxidation peaks are not as well defined as for pure Pt. With reference to Figure 12 (b) in methanol with supporting acid electrolyte, a larger oxidation current is observed for the alloy at the potential at which methanol oxidation occurs on the forward scan but the magnitude of the oxidation current (of methanol's partial oxidation intermediates) produced on the back scan on reduction of the oxidized electrode surface was smaller. Although the potential distribution of the oxidation current was different for the alloy versus pure Pt, the total oxidation current (total area under the peaks) was the same. We are expecting delivery of Os soon, so we shall complete fabrication of remaining electrodes to be studied. Steady-state RRDE studies will be used to identify and quantitatively determine the ratio of various soluble intermediates formed. Although preliminary data has been obtained using H_2SO_4 electrolyte, $HClO_4$ electrolyte will be used for all future electrochemical studies. Use of liquid methanol in a dilute supporting perchloric acid electrolyte along with a standard hydrogen reference electrode (SHE) will provide an experimental arrangement whereby poisoning of the alloy electrocatalyst by either the electrolyte [Parsons, 1988] or leakage from the reference electrode will be minimized.

Although it is not possible to extrapolate from smooth electrodes to small particles dispersed on carbon [Hamnett, 1990], a comparison of smooth electrodes of various

alloy compositions can be very suggestive. Key questions involve the potentials at which water is adsorbed and the potential at which the surface of the electrode is oxidized resulting in long term poisoning. Also, what are the intermediates resulting from the adsorption of methanol prior to water adsorption? How does the alloy composition affect the potentials and structures mentioned? Certainly strong metal support interactions (SMSI) will make extrapolation from smooth electrodes to supported particles difficult, but smooth electrode trends observed when experimentally moving across the compositional surface of a ternary phase diagram can provide suggestions alternative to purely Edisonian choices of compositions for fuel cell membrane electrode assemblies.

References

Appleby, 1993: A.J. Appleby, and F.R. Foulkes, **Fuel Cell Handbook**, Krieger Publishing Company, Malabar, FL, 1993, (a) p. 342, 346; (b) p. 345.

Arico, 1994: A.S. Arico, V. Antonucci, N. Giordano, A.K. Shukla, M.K. Ravikumar, A. Roy, S.R. Barman, and D.D. Sharma, *J. Power Sources*, 50, 1994, 295-309.

Beden, 1987: B. Beden, S. Juanto, J.M. Leger, and C. Lamy, *J. Electroanal. Chem.*, 238, 1987, 323.

Bond, 1987: Bond, G.C., **Heterogeneous Catalysis**, 2nd edition, Oxford Science Publications, Clarendon Press, Oxford, 1987: (a) p. 57, (b) p. 33, (c) p. 35.

Cameron, 1992: D.S. Cameron, G.A. Hards, and D. Thompsett, *Proc. Workshop Direct Methanol-Air Fuel Cells*, Electrochemical Society, Proc. Vol. 92-14, (Eds. A.R. Landgrebe, R.K. Sen, and D.J. Wheeler), 1992, pp. 10-23.

Hamnett, 1990: A. Hamnett, S.A. Weeks, B.J. Kennedy, G. Troughton, and P.A. Christensen, *Ber. Bunsenges. Phys. Chem.*, 94, 1990, 1014.

Hampson, 1979: N.A. Hampson, M.J. Willars, and B.D. McNicol, *J. Power Sources*, 4, 1979, 191.

Hutchinson, 1972: J.M. Hutchinson, *Platinum Metals Review*, 16(3), 1972, 88.

Iwasita-Vielstich, 1990: T. Iwasita-Vielstich, Progress in the study of methanol oxidation by *in-situ*, *ex-situ* and on-line methods, in: *Advances in Electrochemical Science and*

Engineering (Edited by H. Gerischer and Ch. W. Tobias), Vol. 1, Verlag Chemie, Weinham, 1990, pp. 127-170.

Iwasita, 1992: T. Iwasita, F.C. Nart, B. Lopez, and W. Vielstich, *Electrochim. Acta*, 37(12), 1992, 2361.

Landgrebe, 1992: A.R. Landgrebe, and R.K. Sen, *Proc. Workshop Direct Methanol-Air Fuel Cells*, Electrochemical Society, Proc. Vol. 92-14, (Eds. A.R. Landgrebe, R.K. Sen, and D.J. Wheeler), pp. v-xv.

McNicol, 1981: B.D. McNicol, *J. Electroanal. Chem.*, 118, 1981, 71.

Parsons, 1988: R. Parsons, and T. VanderNoot, *J. Electroanal. Chem.*, 257, 1988, 9.

Savitskii, 1989: **Handbook of Precious Metals**, (Eds. E.M. Savitskii, and A. Prince), Hemisphere Publishing Corp., New York, 1989, p. 231.

Wang, 1992: S-R. Wang, and P.S. Fedkiw, *J. Electrochem. Soc.*, 139(9), 1992, 2519.

Watanabe, 1972: M. Watanabe, T. Suzuki, and S. Motoo, *Denki Kagaku*, 40(3), 1972, 205.

Watanabe, 1975: M. Watanabe, and S. Motoo, *J. Electroanal. Chem.*, 60, 1975, 259.

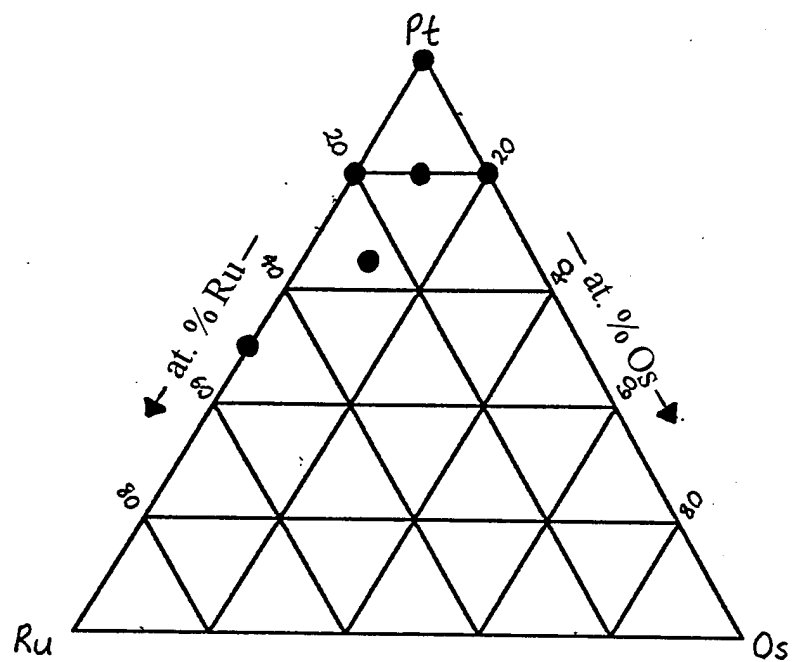Winkler, 1943: O. Winkler, *Z. Electrochem.*, 49, 1943, 221.

Figure 10. Platinum alloy compositions for smooth electrode electrochemical studies.
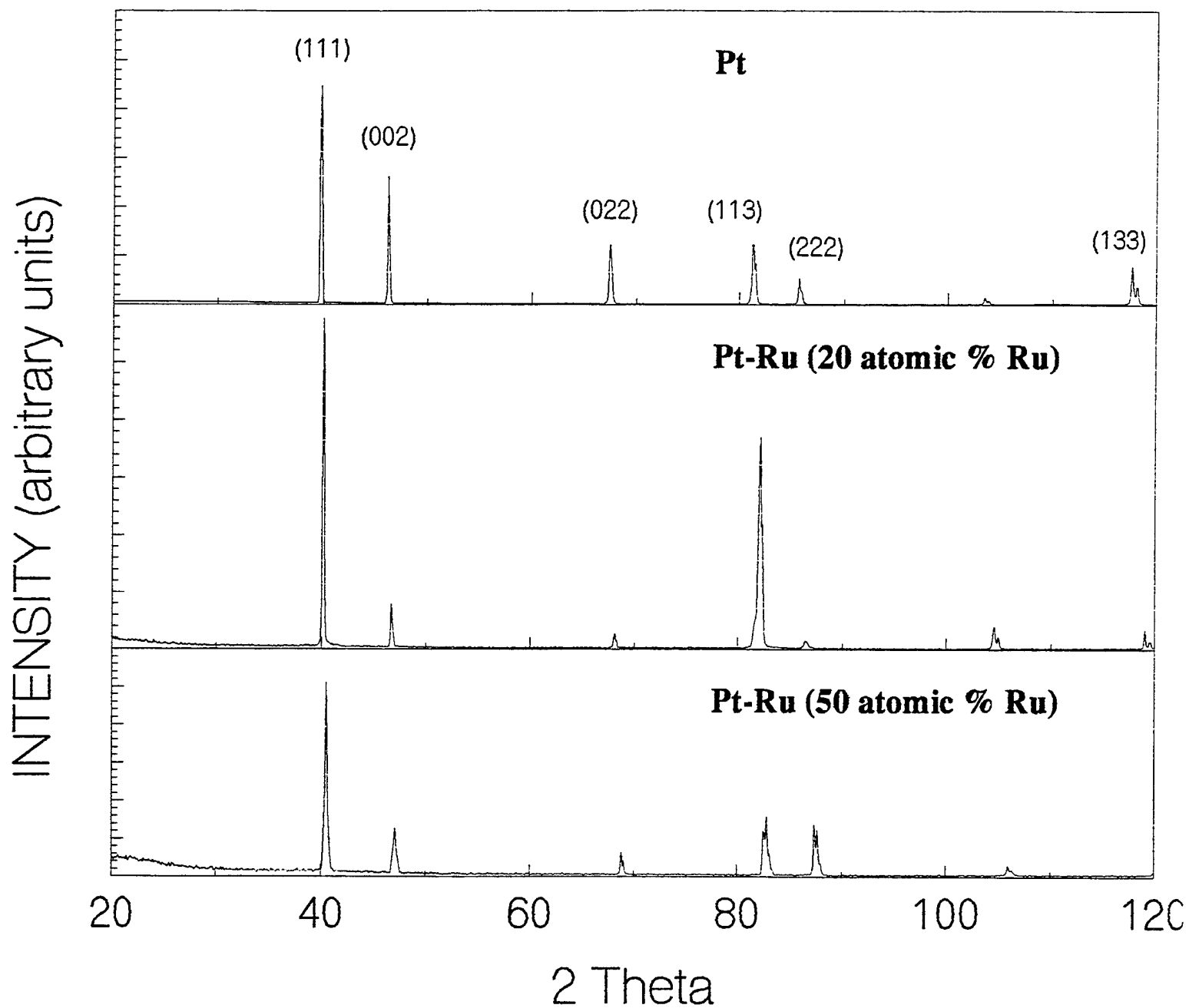
Pt - Ru Alloys

Figure 11. X-ray diffractograms for Pt, Pt-20 at. % Ru, Pt-50 at.%Ru polycrystalline alloys fabricated into disk electrodes.
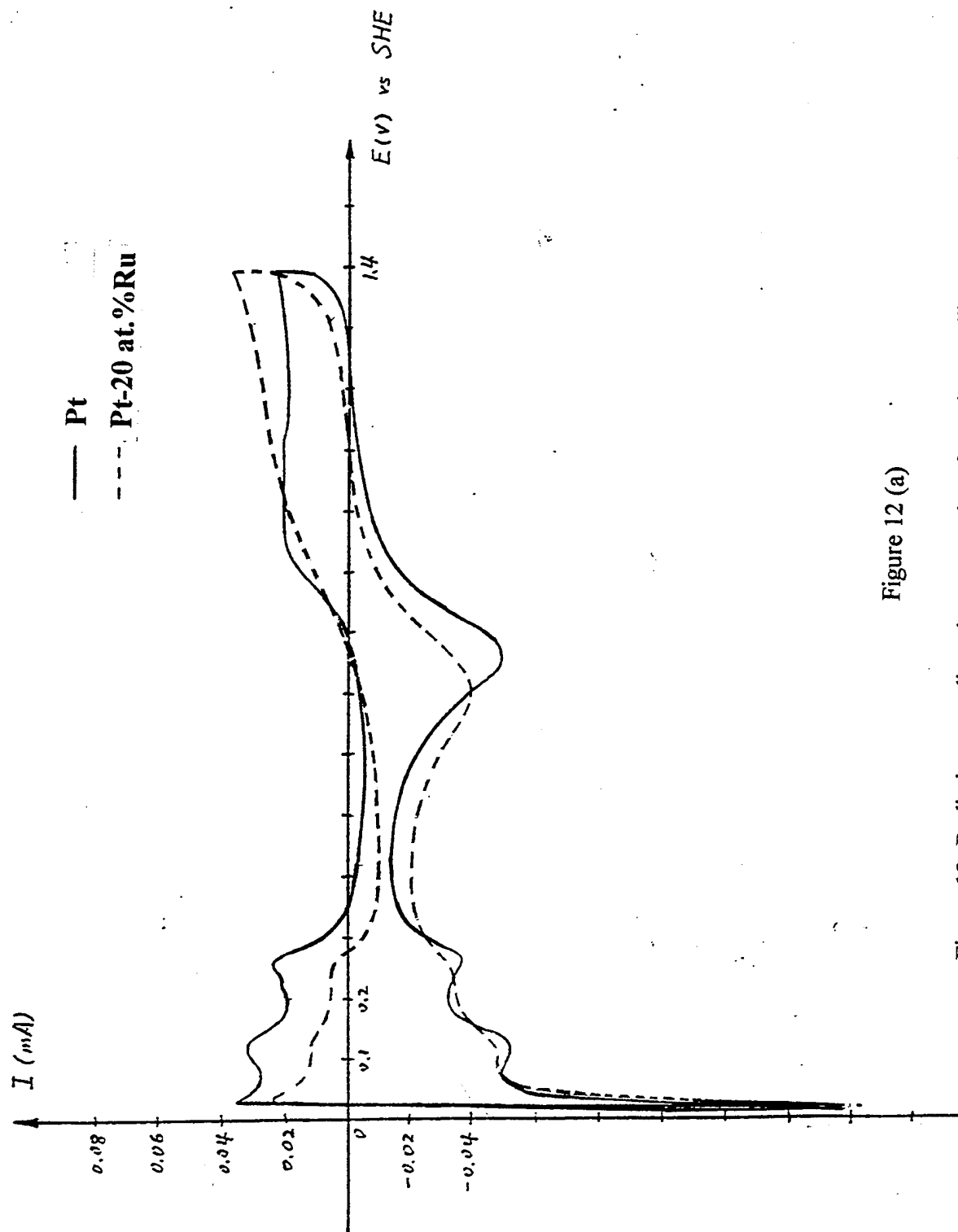
Figure 12. Preliminary cyclic voltammetry data for polycrystalline — Pt, and - - - Pt-20 at.%Ru smooth disk electrodes, in (a) 0.5M H$_2$SO$_4$, and (b) 1M CH$_3$OH, 0.5M H$_2$SO$_4$, solutions respectively.
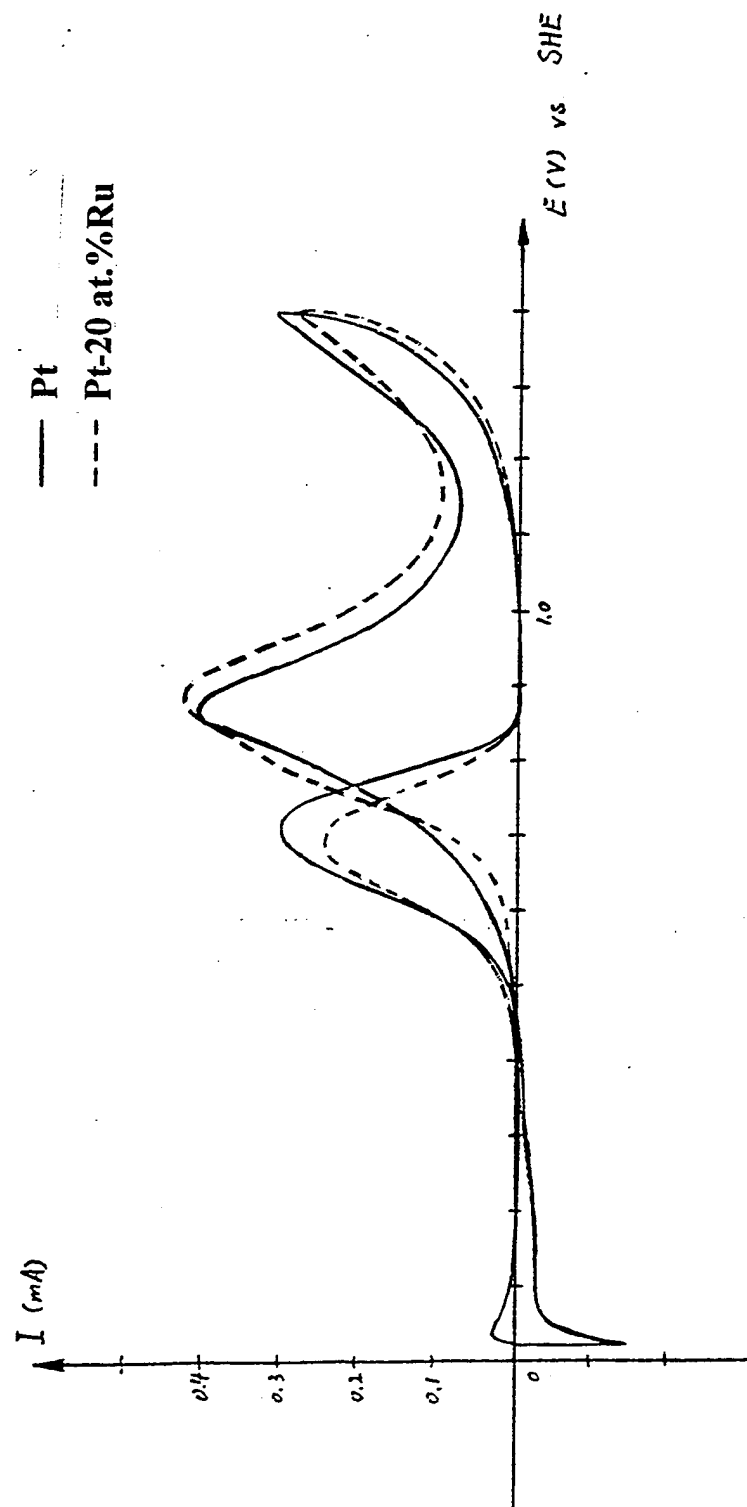
Figure 12 (b)

III. IMPROVED ELECTROCATALYSTS FOR METHANOL ELECTRO-OXIDATION- MEMBRANE ELECTRODE ASSEMBLY HALF-CELL STUDIES

(Lloyd Ploense)

Chromatographic methods development has been performed as of January 17, 1995 for the purpose of obtaining separations between the permanent gas analytes carbon monoxide and carbon dioxide within the half-cell effluent sample matrix. The following summarizes the current instrumentation parameters for the analysis.

Instrument: Perkin-Elmer Auto System Gas Chromatograph with

  Arnell Heated Gas Sampling Valves.

Detector: Thermal Conductivity, Range 3, Temperature 225C.

Injector: Packed Column (1/8 in) Injector, Temperature 190 C.

  1.0 ml Gas Sampling Loop and Valve, Temperature 170 C.

  Gas Sample Injection Interval: 0.1 to 0.3 min.

Column: 6 ft by 1/8 in SS packed with 80/100 mesh Porapak T.

Carrier: Helium at 30 ml/min.

Column

  Oven: Temperature 1:   50 C

    Time 1:   5 min.

    Program Rate: 25 C/min.

    Temperature 2:   180 C

    Time 2:   As Necessary, Typically 30 min.

Integrator/ Data System: Perkin-Elmer 1022 Data Acquisition System.

Employing the above parameters it was determined that carbon monoxide and carbon dioxide had retention times of 0.61 and 1.92 min. respectively. However, although nitrogen, oxygen and hydrogen did not interfere with the carbon dioxide analysis, they were found to coelute with carbon monoxide as positive interferences in the first two cases and as a negative interference in the last. Attempts to resolve carbon monoxide from oxygen and nitrogen by lowering the initial isothermal temperature for the chromatography to the practical minimum of 35 C (without LN_2 subambient techniques), decreasing the detector signal filter frequency and setting the integration peak width to it's minimum did not improve carbon monoxide/nitrogen/oxygen resolution. Since further method development employing multiple columns and column switching valves would be required to obtain complete separation of all the possible interferences from carbon monoxide while retaining the capability to analyze the other components of interest in the sample matrix; formaldehyde, methanol, methyl formate, dimethylacetyl formaldehyde (methylal) and formic acid, methods for exclusion of the interferences from the sample stream were chosen over more complex chromatography.

Modifications of the process/sampling pneumatics have been made which permit continuous operation of the half-cell during gas phase calibration of the analytical instrumentation. These modifications permit continuous maintenance of a helium flow through the apparatus effectively minimizing contamination of the sample stream by atmospheric interferences (Figure 13). In addition provisions have been made for sampling system blanks to be analyzed to ensure that there are no residual analytes or

27

aforementioned modifications to provide for head space gas phase injections of the liquid analytes and suspect additional components to assist retention time peak identification methodology by eliminating the syringe injection/gas sampling loop retention time discrepancies.

Procedures for automated effluent analysis and GC data collection have been initiated which will allow greatly enhanced data collection capability particularly as stability/depletion (or poisoning) studies of the catalyst/membrane pairs for long time periods are conducted.

In combination the system modifications permit experimental runs of long duration with analytical data collection intervals limited only by the length of the gas chromatographic temperature program. Calibration of the analysis and sampling system blanks can now be conducted without interruption of the half cell process resulting in data of increased reproducibility.
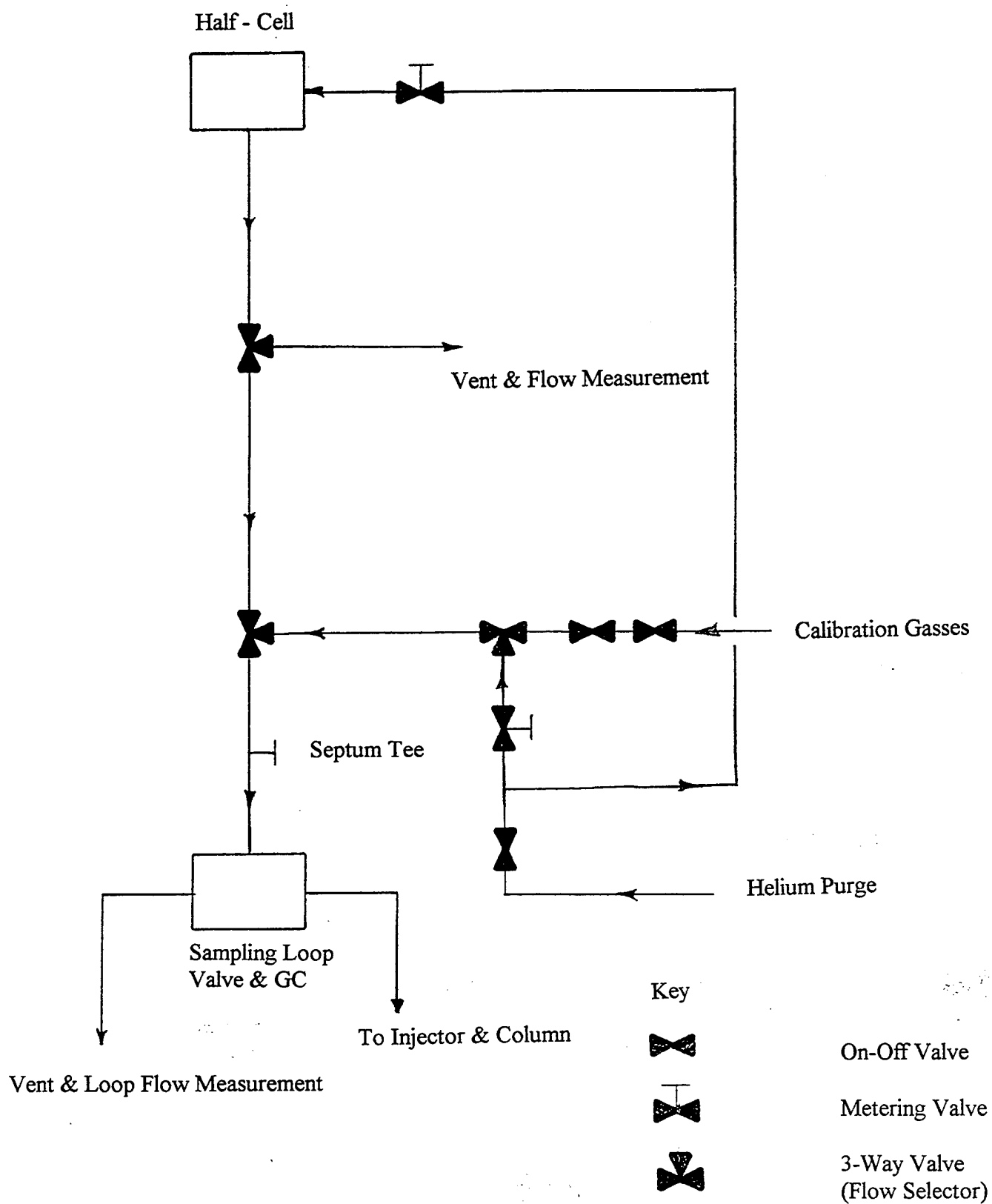
Half - Cell

Vent & Flow Measurement

Calibration Gasses

Septum Tee

Helium Purge

Sampling Loop
Valve & GC

To Injector & Column

Vent & Loop Flow Measurement

Key

On-Off Valve

Metering Valve

3-Way Valve
(Flow Selector)

Figure 13

29

IV. X-RAY STUDIES OF ANODE CATALYTIC MATERIALS FOR DIRECT METHANOL FUEL CELLS

(Argonne National Laboratory: D. Zurawski and A. Aldykiewicz)

During this first quarter of the Hub program, the effort at Argonne National Laboratory has been less than anticipated due to delays in establishing the subcontract between Illinois Institute of Technology and Argonne National Laboratory.

A postdoctoral appointee has been hired. He has expertise in both electrochemistry and in situ X-ray absorption characterization of electrochemical systems. He is also knowledgeable in the operation of a synchrotron beamline since his graduate studies were performed at the National Synchrotron Light Source at Brookhaven National Laboratory.

We have developed expertise in the fabrication of membrane-electrode assemblies by the state-of-the art ink technique which will be utilized for the in situ X-ray studies. Progress has been made towards improving the power output of the membrane-electrode assemblies. Also, a general user proposal has been submitted to the National Synchrotron Light Source for beamtime in additional to that which will be purchased. The proposal has been accepted and we have received twelve days of beamtime distributed over the next two years. Additional beamtime will be requested by submission of an extension proposal during January, 1995. The first allocation of beamtime will be three days in March, 1005. Experiments planned for these first three days are ex situ X-ray absorption measurements on the platinum and platinum-ruthenium catalysts and preliminary in situ absorption measurements. The purpose of the ex situ experiments is to determine the effect of the carbon support and the addition of experiments will demonstrate the feasibility of the X-ray/electrochemical cell design for obtaining absorption data.

A meeting with researchers from the groups of James McBreen (Brookhaven National Laboratory) and William O'Grady (Naval Research Laboratory) is planned for early January to discuss research plans that can be mutually beneficial.

V. Minority Institute Fuel Cell/Battery Workshop

On December 16- 20, 1994 a workshop was held at IIT.

Instructors: Profs. Eugene S. Smotkin and J. Robert Selman

Organization: Wendy Zhang (Administrative Associate)

Laboratory Assistants: Rexuan Liu, Josh Mackenzie

Ching-Chih Li

Attended by:

Professor Vijay K. Gupta, Central State University

Dr. Michael May Postdoctoral Fellow

Professor Justin Akujieze, Chicago State University

Professor Dieg Sandoval, Pan American University

Mr. Frank Perales

A series of lectures on batteries and fuel cells were held as well as experiments conducted on equipment purchased for the minority institute educational labs. Details of this workshop will be included in the annual report.